Romanian Reports in Physics, Vol. 66, No. 4, P. 1002–1011, 2014

OPTICAL AND ELECTRICAL PROPERTIES OF ZnSe THIN FILMS: EFFECT OF VACUUM ANNEALING

JEEWAN SHARMA[1*], DEEP SHIKHA[2, 3], S.K. TRIPATHI[4]

[1] Sri Guru Granth Sahib World University, Department of Nanotechnology, Fatehgarh Sahib, (India)
E-mail: jeewansharma29@gmail.com
[2] Maharishi Markandeshwar University, Department of Physics, Mullana, Ambala - 133207, (India)
E-mail: deep_shikha79@yahoo.co.in
[3] Ambala College of Engineering and Applied Research, Mithapur-133101 (India)
[4] Panjab University, Centre of Advanced Study in Physics, Chandigarh - 160 014, (India)

Received September 25, 2013

Abstract. Inert gas condensation method has been successfully employed for depositing ZnSe thin films. These films have been deposited at argon gas partial pressure of 2×10^{-1} mbar and room temperature (298 K). After deposition these films have been annealed (in vacuum at 473 K) for one hour. The optical and electrical properties of these films have been investigated before and after annealing using optical transmission and conductivity measurements. The absorption coefficient (α) and band gap (E_g) are calculated using transmission curves. Optical transmittance measurements indicate the existence of direct allowed optical transition with a corresponding energy gap in the range of 2.80–3.00 eV. The dark conductivity (σ_d) and photoconductivity (σ_{ph}) measurements, in the temperature range 253–358 K, indicate that the conduction in these materials is through an activated process having two activation energies. σ_d and σ_{ph} values increase with the annealing. The values of carrier life time have been calculated and these values increase with the increase in the crystallite size on annealing. Thermal treatment has appreciable effect on above mentioned properties.

Key words: inert gas condensation, vacuum annealing, activation energy.

1. INTRODUCTION

ZnSe is group II-VI semiconductors having a direct optical band gap of about 2.7 eV [1–2]. This material has many attractive properties. Its large band gap, low resistivity, remarkable photosensitivity makes it suitable for a variety of the optoelectronic applications in the blue green wavelength region, including light emitting diodes and lasers [3–8]. Due to its wide band gap and transparency over a wide range, it is suitable for window layer for solar cells [9]. Further, it is also used to produce optical elements (windows, lenses, prisms) for IR range including the passive laser optics elements. It has superior optical transmission with extremely

low bulk losses from scattering and absorption. The effect of different deposition parameters such as pressure, substrate temperature, pH and annealing on properties of ZnSe is an area of interest these days [10]. Due to its interesting physical properties and device applications a variety of techniques have been used for the deposition of ZnSe films. Some of these techniques are MOCVD [11], RF magnetron sputtering [12], molecular beam epitaxy [13], MOVPE and Inert gas condensation (evaporation in presence of inert gas) [14]. The knowledge of structural, optical and electrical properties of ZnSe films is very important for such applications. In the present work, Inert gas condensation technique is used to prepare the ZnSe thin films, because this technique is relatively simple, inexpensive and convenient, in particular for large area deposition. The present paper describes the effect of vacuum annealing on optical and electrical properties of ZnSe films.

2. EXPERIMENTAL DETAILS

Melt-quenching technique was used to prepare semiconducting $Zn_{25}Se_{75}$ from its constituents (5N pure) [15]. Thin films of this material were grown in a conventional vacuum coating system on well degassed chemically cleaned Corning 7059 glass substrates. The vacuum chamber was evacuated to 2×10^{-6} mbar and Ar gas was introduced through specially designed inlet tube having a jet of diameter ~ 0.5 mm. This jet was kept adjacent to the evaporation boat pointing towards the glass substrates. The vacuum chamber was purged several times with spectroscopic grade Ar gas to remove any residual gas impurities. Thermal evaporation of the material was carried out from the Mo boat in the presence of Ar gas partial pressure of 2×10^{-1} mbar. After deposition this film was annealed at 473 K for one hour in vacuum of 2×10^{-3} mbar. A double beam spectrophotometer [HITACHI-330] was used to study the optical transmission in ZnSe thin films. Electrical measurements of these thin films were carried out in a specially designed metallic sample holder where heat filtered white light of intensity 8450 Lux (200 W tungsten lamp) was shown through a transparent glass window. A vacuum of about 10^{-3} mbar was maintained throughout these measurements. Light intensity was measured using a digital luxmeter (*MASTECH*, MS6610). Planar geometry of the films (length ~ 1.0 cm; electrode gap ~ 8×10^{-2} cm) was used for the electrical measurements. Pre deposited thick Indium electrodes were used for the electrical contacts. The electrical conductivity in thin film was calculated using two probe method. The photocurrent (I_{ph}) was obtained after subtracting the dark current (I_d) from the current measured in the presence of light. For transient photoconductivity measurements, light was shone on the thin film for 90 seconds and then switched off. The rise and decay of photocurrent was noted manually from a digital picoammeter (DPM-11 Model). The accuracy in I_{ph} measurements was typically 1 pA.

3. RESULTS AND DISCUSSION

Fig. 1(i) shows the transmission spectra of as-deposited and annealed thin films. From the transmission data, nearly at the fundamental absorption edge, the values of absorption coefficient (α), are calculated the relation (1) and shown in Fig. 1(ii).

$$\alpha = \frac{1}{d}\ln\left(\frac{1}{T}\right). \tag{1}$$

To see the nature of transition in ZnSe, the variation of d{ln($\alpha h\nu$)}/d($h\nu$) w.r.t. $h\nu$ is studied [16]. Fig. 2(i) shows the plots of d{ln($\alpha h\nu$)}/d($h\nu$) vs hν, for as-deposited and annealed thin films, with discontinuities at 2.95 eV and 2.21 eV respectively.

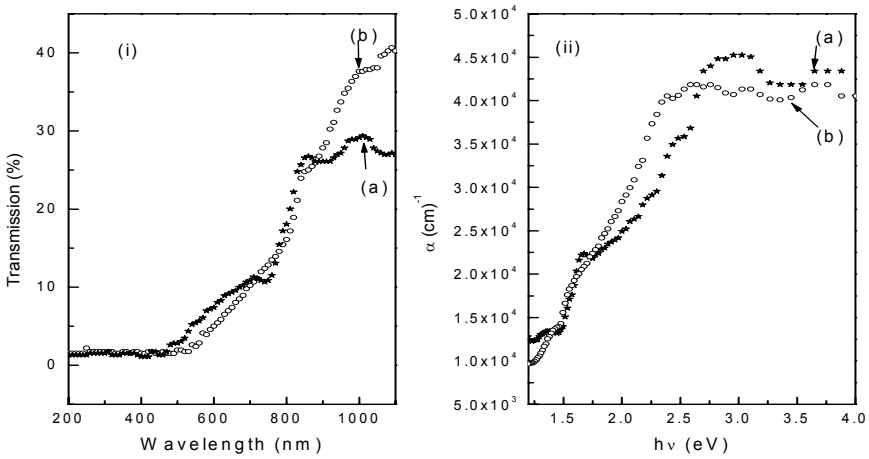

Fig. 1 – Transmission spectra (i) and absorption coefficients (ii) of as-deposited (a) and annealed ZnSe thin films (b).

Taking these values as the optical gap of ZnSe thin films, ln($\alpha h\nu$) *vs*. ln($h\nu$–E_g) graphs are plotted. From the slopes of these straight line graphs (Fig. 2(ii)), values of n have been calculated, which comes out to be 0.45 and 0.35 respectively. These values are close to 0.5 indicating that the transition is direct. The values of optical gap were calculated using the straight line portion of $(\alpha h\nu)^{1/n}$ vs. $h\nu$ graphs taking $n = 0.5$.

Figure 3 shows the plots of $(\alpha h\nu)^2$ *vs*. hν for as-deposited and annealed thin films. The experimental values of the optical gap calculated from the figure are (3.00 ± 0.01) eV for as-deposited and (2.80 ± 0.01) eV for annealed thin films. There is a red shift of 0.20 eV in the optical gap after annealing the film. This

shows that the improvement in crystallinity is followed by a shift in the optical absorption edge of the films towards lower energy values. The increase in crystallinity on annealing ZnSe thin films at 473 K for 15 minutes was also reported previously [10].

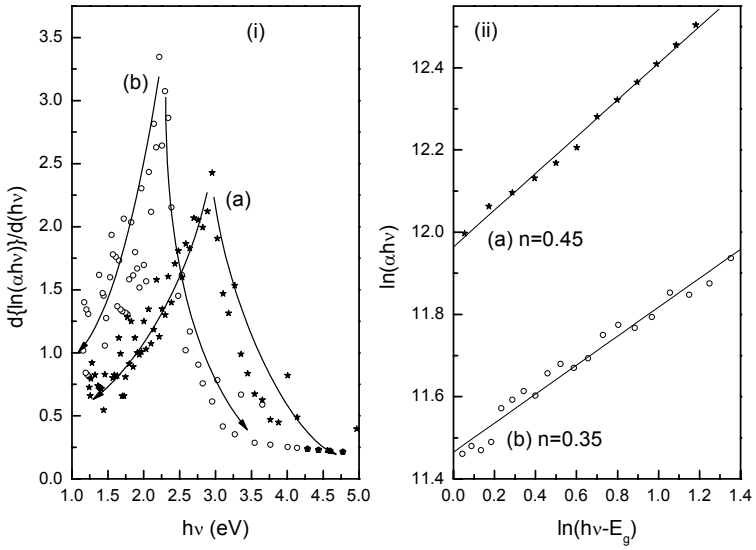

Fig. 2 – Variation of d{ln(α*h*ν)}/d(*h*ν) with energy (i) and plots of ln (α*h*ν) *vs*. ln(*h*ν–*Eg*) (ii) for as-deposited (a) and annealed ZnSe thin films (b).

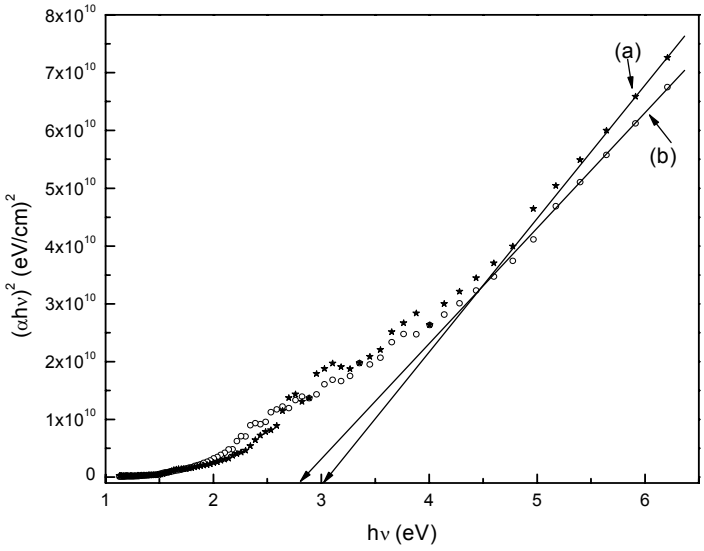

Fig. 3 – Variation of $(\alpha h\nu)^2$ with energy for as-deposited (a) and annealed ZnSe thin films (b).

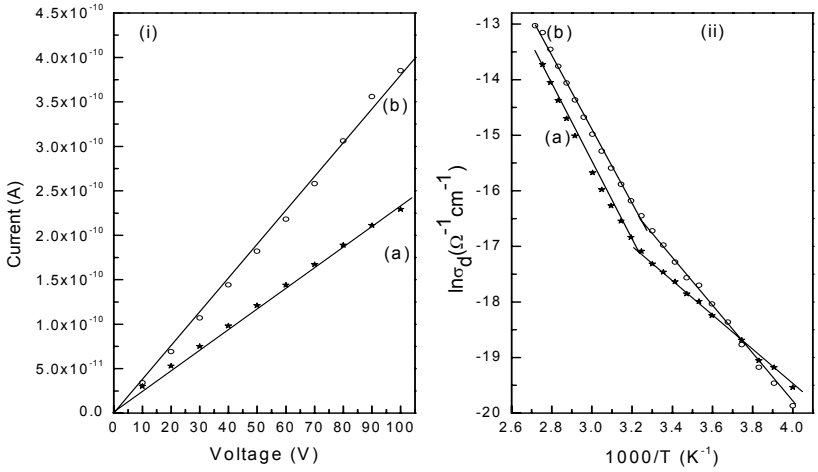

Fig.4 – *I-V* plots (i) and temperature dependence of dark conductivity (ii) for as-deposited (a) and annealed ZnSe thin films (b).

Figure 4(i) shows the current *vs*. voltage plots for as-deposited and annealed ZnSe thin films. The *I-V* curves are found to be symmetric and linear upto the operating range of applied voltage. The electrical conductivity shows typical Arrhenius type of activation

$$\sigma_d = \sigma_o \exp\left(\frac{-\Delta E}{kT}\right), \tag{2}$$

where ΔE is the activation energy for conduction and k is the Boltzmann's constant. The values of σ_d for as-deposited and annealed ZnSe thin films are found to be $(2.19 \pm 0.02)\times10^{-8}$ Ω^{-1}cm^{-1} and $(4.23 \pm 0.02) \times10^{-8}$ Ω^{-1}cm^{-1} respectively at 298 K. These values of conductivity are in good agreement with earlier reported values [17–18]. Figure 4(ii) shows the temperature dependence of dark conductivity for as-deposited and annealed ZnSe thin films in the temperature range 250–370 K. The plots of $\ln\sigma_d$ *vs*. $1000/T$ have two linear portions. First in the lower temperature range (250–315 K), characterized by a small slope and second in higher temperature range (315–370 K) having large slope. The activation energies for dc conduction have been calculated from the slopes of $\ln\sigma_d$ *vs*. $1000/T$ curves for both lower and higher temperature ranges. The temperature dependence of the conductivity at lower temperature in the range can be attributed to extended state conduction mechanism. In higher temperature range the electronic transport properties of thin semiconductor films are strongly influenced by their structural characteristics (the crystallite shape and size, inter crystal boundaries, lattice defects, etc.) and purity (nature and concentration of the impurities, adsorbed and

absorbed gases, etc.). So, the conduction mechanism in ZnSe thin film samples can be explained on the basis of the Seto's model with several modifications proposed by Baccarani *et al*. [19].

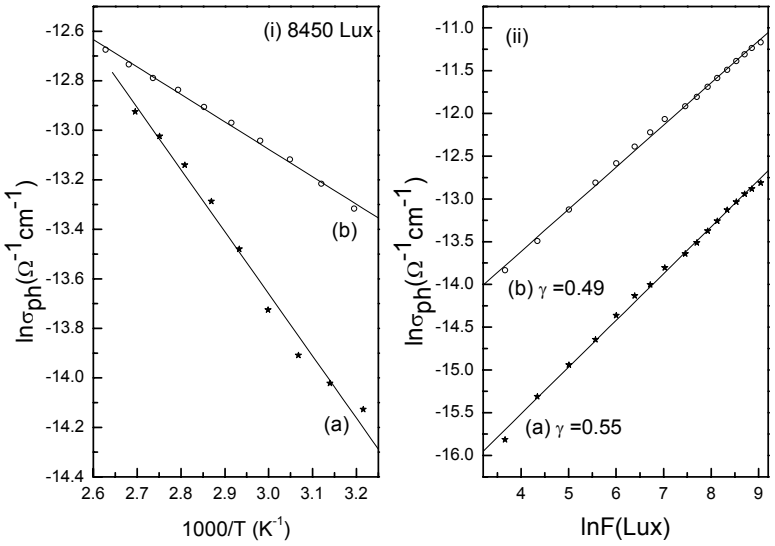

Fig. 5 – Temperature (i) and intensity dependence of photo conductivity (ii) for as-deposited (a) and annealed ZnSe thin films (b).

The values of σ_d and ΔE_d are given in Table 1. The value of σ_d increases and ΔE_d decreases on annealing ZnSe thin film. This type of behavior has also been observed by others for semiconductors [20–21]. The increase in electrical conductivity and decrease in activation energies after annealing may be due to the change in crystal structure (improvement in crystallite and grain size), decrease in inter-crystallite boundaries (grain boundary domains) and removal of some impurities (adsorbed and absorbed gases). Excess atoms of compound are also possible [22] due to a small change in stoichiometry after annealing.

Figure 5 (i) shows the temperature dependence of photoconductivity for as-deposited and annealed ZnSe thin films. The values of photoconductivity are calculated to be $(9.42 \pm 0.02)\times10^{-7}$ $\Omega^{-1}cm^{-1}$ and $(2.85 \pm 0.02)\times10^{-6}$ $\Omega^{-1}cm^{-1}$ for as-deposited and annealed ZnSe thin films at 298 K. Clearly, the value of σ_{ph} increases on annealing. The photo activation energy has been calculated using the slopes of Fig. 5 (i) and is found to decrease from (0.22 ± 0.01) eV to (0.10 ± 0.01) eV on annealing (Table 1). The activation energies for photoconduction are much smaller than for the dark conduction. No maximum in the steady state photoconductivity with temperature has been observed in the measured temperature range. Photosensitivity is found to increase after annealing.

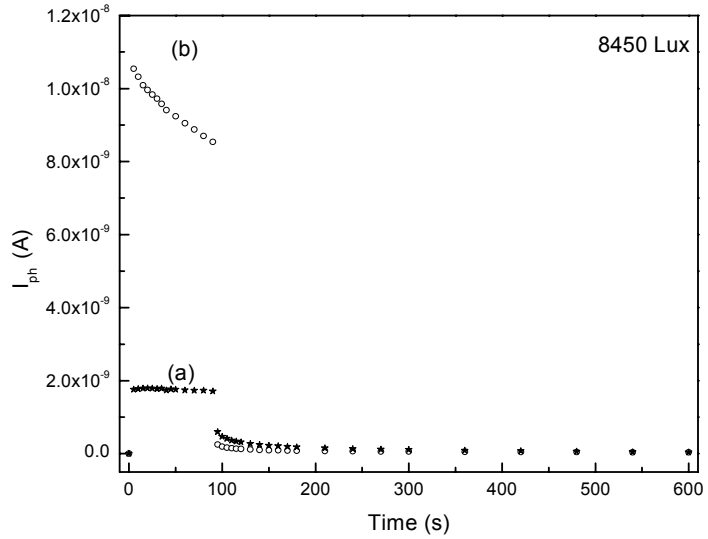

Fig. 6 – Rise and decay of photocurrent for as-deposited (a) and annealed ZnSe thin films (b).

Figure 5 (ii) shows the intensity dependence of σ_{ph} for as-deposited and annealed ZnSe thin films. It is clear from the figure that $\ln\sigma_{ph}$ vs. $\ln F$ curves are straight lines indicating that the σ_{ph} follows a power law with intensity (F), i.e., $\sigma_{ph} \propto F^{\gamma}$. In as-deposited and annealed ZnSe thin films, the values of γ are found to be in between 0.5 and 1.0, indicating that the resulting recombination mechanism is bi-molecular [23], where the recombination rate of electrons is proportional to the number of holes. Photosensitivity (σ_{ph}/σ_d) of the order of $10–10^2$ has been found in ZnSe thin films.

Figure 6 shows the rise and decay curves of I_{ph} for as-deposited and annealed ZnSe thin films. I_{ph} rises to a steady state value and no peak is observed for as-deposited film while a peak is observed in rise curve of annealed ZnSe film. It is evident that decay of I_{ph} is slow. In materials, having traps in the mobility gap, the recombination time of carriers is same as carrier life time when free carrier density is more than trapped carrier density [24]. If the free carrier density is much less than the trapped carriers, then the recombination process is dominated by the rate of trap emptying and is much larger than carrier life time, resulting in a slow decay. During decay, the photocurrent does not reach zero for a long time after the incident light is switched off. A persistent photocurrent is observed in all the cases. This type of photoconductive decay has also been reported in various other semiconductors [25–27]. In the present case, non-exponential decay of photocurrent is observed. The values of τ_d at different times have been calculated using.

$$\tau_d = -\left[\frac{1}{I_{ph}}\left(\frac{\mathrm{d}I_{ph}}{dt}\right)\right]^{-1} \tag{3}$$

for as-deposited and annealed ZnSe thin films from the slopes (at different times) of decay curves of Fig. 6.

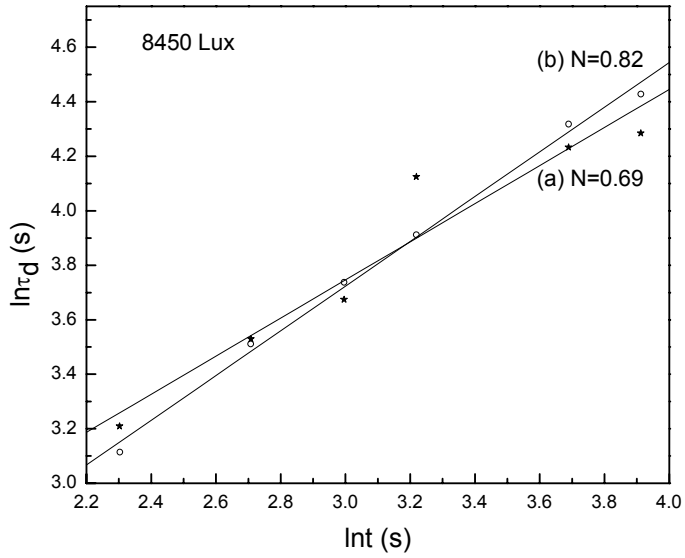

Fig. 7 – Plots of $\ln\tau_d$ *vs*. $\ln t$ for as-deposited (a) and annealed ZnSe thin films (b).

The decay times observed for ZnSe thin films are found to be time dependent. The value of τ_d increases with time, which confirms the non-exponential decay of photocurrent. Fig. 7 shows the plots of $\ln\tau_d$ vs. $\ln t$ for as-deposited and annealed ZnSe thin films at a temperature 298 K and intensity 8450 Lux. The extrapolation of the curves at $t = 0$, give the values of the carrier life time [28] and are found to be 1.6 and 1.3 seconds for as-deposited and annealed ZnSe thin films respectively. Clearly, the carrier life time decreases on annealing the film. The straight lines in Fig. 7, obey a power law of the form t^{-N}, with $N = \mathrm{d}(\ln\tau_d/\ln t)$ and the values of N are 0.69 and 0.82 for as-deposited and annealed ZnSe thin films.

Table 1

Optical and electrical parameters of ZnSe thin films before and after annealing

	Band Gap (eV)	σ_d (Ω^{-1} cm^{-1})	σ_{ph} (Ω^{-1} cm^{-1})	ΔE_d (eV)		ΔE_{ph} (eV)	γ	τ_d (sec)	Carrier life time (s)
				*LTR	HTR				
Before Annealing	3.00	2.19×10^{-8}	9.42×10^{-7}	0.28	0.63	0.22	0.55	24.8	1.60
After Annealing	2.80	4.23×10^{-8}	2.85×10^{-6}	0.39	0.59	0. 10	0.49	22.5	1.30

* LTR = Low temperature range; HTR = High temperature range

4. CONCLUSIONS

The ZnSe thin films were deposited on well degassed corning glass substrates using inert gas condensation technique. The transition in the films was found to be direct. The optical band gap value decreases after annealing. The value of σ_d increases and ΔE_d decreases after thermal annealing. *I-V* curves are symmetric and linear up to the operating range of applied voltage. Steady state photoconductivity studies indicate that there is continuous distribution of localized states. Decay of photocurrent is non-exponential and slow which may be due to the presence of deeper localized states in this material. The value of decay time constant increases with time, confirming the non-exponential decay of photocurrent. The carrier life time is found to decrease with annealing.

Acknowledgements. The experimental work has been performed in Department of Physics, Panjab University Chandigarh. We acknowledge the financial support provided by the CSIR, New Delhi for the completion of this work.

REFERENCES

1. K. R. Murali, S. Dhanapandiyana and C. Manoharana, Chalcognite letters, **6**, *1*, 51–56 (2009).
2. S. Antohe, L. Ion, Mihaela Girtan and O. Toma, Romanian Reports in Physics, **65**, *3*, 805–811 (2013).
3. Y. Araki, K. Ohkuno, T. Furukawa and J. Saraie, Journal of Crystal Growth, **301–302**, 809–811 (2007).
4. T. Shirakawa, Mater. Sci. and Engin. B, **91–92**, 470–475 (2002).
5. T. Nakamura, K. Katayama, H. Mori and S. Fujiwara, Physica Status Solidi (b), **241**, *12*, 2659–2663 (2004).
6. Y. Jiao, D. Yu, Z. Wang, K. Tang and X. Sun, Materials Letters, **61**, *7*, 1541–1543 (2007).
7. S. Venkatachalam, R. Kumar, D. Mangalaraj, S. K. Narayandass, K. Kim and J. Yi Solid-State Electronics, **48**, *12*, 2219–2223 (2004).
8. D. S. Patil and D. K. Gautam Optics Commun., **201**, *4–6*, 413–423 (2002).
9. S. Armstrong, P. K. Datta and R. W. Miles, Thin Solid Films, **403–404**, 126–129 (2002).
10. A. P. Samatilleke, M. H. Boyle, J. Young and I. M. Dharmadasa, J. Mater. Sci.: Mater Electro., **9**, *3*, 231–235 (1998).
11. Y. Noda, T. Ishikawa, M. Yamabe and Y. Hara, Appl. Surf. Sci., **113–114**, 28–32 (1997).
12. A. Rizzo, M. A. Tagliente, L. Caneve and S. Scaglione, Thin Solid Films, **368**, 8–14 (2000).
13. T. W. Kim et al., Thin Solid Films, **298**, *1–2*, 187–190 (1997).
14. M. El. Sherif, F. S. Terra and S. A. Khodier, J. Mater. Sci.Mater.Electron., **7**, *6*, 391–395 (1996).
15. A. Thakur, V. Sharma, G. S. S. Saini, N. Goyal and S. K. Tripathi, J. Phys D: Appl. Phys., **38** 1959–1965 (2005).
16. J. Sharma, G. S. S. Saini, N. Goyal and S. K. Tripathi, Journal of Optoelectronics and Advanced Materials, **9**, *10*, 3194–3199 (2007).
17. R. B. Kale and C. D. Lokhande, Materials Research Bulletin, **39**, *12*, 1829–1839 (2004).
18. J. Krustok and P. E. Kukk, Materials Science, **15**, 43–55 (1989).
19. J. Sharma and S.K. Tripathi, Physica B, **406**, *9* 1757 (2011).
20. R. B. Kale and C. D. Lokhande, Appl. Surf. Sci., **223**, *4*, 343–351 (2004).
21. R. B. Kale and C. D. Lokhande, Semicond. Sci. Technol., **20**, *1*, 1–9 (2005).

22. S. Ghosh, A. Mukherjee, H. Kim and C. Lee, Materials Chemistry and Physics, **78**, *30*, 726–733 (2003).
23. A. Rose, *Concepts in Photoconductivity and Allied Problems*, Interscience, New York, 1963.
24. M. Igalson, Solid State Communications, **44**, *2*, 247–250 (1982).
25. V. Sharma, A. Thakur, P. S. Chandel, N. Goyal, G. S. S. Saini and S. K. Tripathi, J. Optoelect. Adv. Mater., **5**, *5*, 1243–1248 (2003).
26. D. V. Harea, I. A. Vasilev, E. P. Colomeico and M. S. Iovu, J. Optoelect. Adv. Mater., **5**, *5*, 1115–1120 (2003).
27. M. S. Iovu, S. D. Shutov, V. I. Arkhipov and G. J. Adriaenssens, J. Non-Cryst. Solids, **299–302** 1008–1012 (2002).
28. D. P. Padiyan, A. Marikani and K. R. Murali, Cryst. Res. Technol., **35**, *8*, 949–957 (2000).